



The effect of electrolyte composition on the plasma electrolyte oxidation and phase composition of oxide ceramic coatings formed on 2024 aluminium alloy






V.M. Posuvailo ^a, V.V. Kulyk ^{b,*}, Z.A. Duriagina ^{b,c},
I.V. Koval'chuck ^a, M.M. Student ^a, B.D. Vasylyv ^a

^a Karpenko Physico-Mechanical Institute of the National Academy of Sciences of Ukraine, 5 Naukova St., Lviv, 79060, Ukraine

^b Lviv Polytechnic National University, 12 Bandera St., Lviv, 79013, Ukraine

^c The John Paul II Catholic University of Lublin, Raclawickie 14 Ave., 20-950 Lublin, Poland

* Corresponding e-mail address: kulykvolodymyrvolodymyrovych@gmail.com

ORCID identifier:  <https://orcid.org/0000-0003-0998-7588> (V.M.P.);  <https://orcid.org/0000-0001-5999-3551> (V.V.K.);  <https://orcid.org/0000-0002-2585-3849> (Z.A.D.);  <https://orcid.org/0000-0002-5992-5898> (M.M.S.);  <https://orcid.org/0000-0002-8827-0747> (B.D.V.)

ABSTRACT

Purpose: Purpose of this work is to analyse the process of synthesis of oxide ceramic coatings in plasma electrolytes on 2024 aluminium alloy and to form an electrolyte which allows to reduce energy consumption for the coating formation.

Design/methodology/approach: The oxide ceramic coatings were synthesized on 2024 aluminium alloy. The coatings were formed by the alternate application of anode and cathode pulses to the sample. X-ray diffraction analysis of coatings was performed on a DRON-3.0 X-ray diffractometer using CuK_α radiation. The thickness of the coatings was determined using a CHY TG-05 thickness gauge. The porosity of the coatings was investigated by analysing the micrographs of the plasma electrolyte oxidation (PEO) coatings obtained on a scanning electron microscope at $\times 500$ magnification using the image processing technique.

Findings: The electrolyte with 5 g/l H_2O_2 additive have been elaborated as an optimal composition for synthesis of a coating with an increased content of corundum ($\alpha\text{-Al}_2\text{O}_3$) as compared to a coating synthesized in the same mode in the $3\text{KOH}+2\text{Na}_2\text{SiO}_3$ electrolyte without H_2O_2 . This synthesis mode allows obtaining a coating with a high corundum content at low energy consumption.

Research limitations/implications: For further optimization of the synthesis modes, it is necessary to analyse the influence of the phase composition and porosity of the obtained oxide ceramic coatings on their microhardness, wear resistance, and corrosion resistance.

Practical implications: Based on the developed modes of synthesis of the coatings, it will be possible to obtain wear and corrosion resistant oxide ceramic coatings with predetermined functional properties and to reduce energy consumption for their formation.

Originality/value: Methods for accelerating the formation of coatings have been proposed and tested, in particular, by adding various amounts of hydrogen peroxide to the electrolyte. The content of oxides in the obtained coatings, in particular, their ratios at various concentrations of hydrogen peroxide in the electrolyte, were determined by X-ray phase analysis. The modes of synthesis of the coatings were developed which allow obtaining a continuous coating without cracks with simultaneous decreasing porosity from 4.32% to 3.55–3.53%.

Keywords: Plasma electrolyte synthesis, Microstructure, Plasma electrolyte oxidation, Hydrogen peroxide, Porosity

Reference to this paper should be given in the following way:

V.M. Posuvailo, V.V. Kulyk, Z.A. Duriagina, I.V. Koval'chuck, M.M. Student, B.D. Vasylyv, The effect of electrolyte composition on the plasma electrolyte oxidation and phase composition of oxide ceramic coatings formed on 2024 aluminium alloy, Archives of Materials Science and Engineering 105/2 (2020) 49-55. DOI: <https://doi.org/10.5604/01.3001.0014.5761>

MATERIALS

1. Introduction

Aluminium, magnesium, and titanium alloys are widely used in industry. They significantly reduce the weight of constructions, well absorb shock and vibrations, but their wear and corrosion resistance should be improved by additional surface treatment. The development of new eco-friendly technologies of highly efficient and reliable coatings for the protection and reinforcement of metal ware is one of the most urgent tasks of modern science and technology because of increasing of harshness of operational conditions, especially, action of aggressive technological environments, and corresponding increasing of requirements to structural materials.

There are many ways to increase the wear and corrosion resistance of alloys: anodizing, chromium plating, phosphating, oxidizing, nitrating, etc. [1-6]. All of them increase the corrosion resistance, but the wear resistance of the obtained coatings is insufficient. Nowadays, a relatively new type of surface treatment and reinforcement of metals is actively developing. A new developed plasma electrolyte oxidation (PEO) technique is based on a traditional anodizing process [7-11]. It allows to obtain multifunctional oxide ceramic coatings with a unique complex of properties on valve metals (Al, Mg, Ti, Zr, Ta) [12-15].

Samples of valve metals are immersed in the electrolyte where anode and cathode voltage is alternately applied. There are four main stages of formation of oxide ceramic coatings on valve metals: formation of the primary oxide film by an electrochemical mechanism in the pre-spark stage; the breakdown of the primary oxide film and the appearance of a plasma clot in the discharge channel; gas-phase chemical reactions of formation of intermediate and final product; condensation and polymorphic transformations of oxide phases [16, 17].

The coatings mainly consist of high-temperature oxide phases (Al_2O_3 , TiO_2 , MgO , ZrO_2). In particular, $\alpha\text{-Al}_2\text{O}_3$ coatings with corundum structure formed on aluminium alloys at high temperature have high microhardness (20 GPa) and wear resistance [18,19]. These coatings are wear, corrosion, and heat resistant, and have electrical insulating properties.

Dissociation and thermal decomposition of water occur in the discharge channels by reactions:



These reactions are quite energy-consuming and give the major contribution of O_2 , O , OH^- and OH which the coating is formed of. It was found in [20] that the amount of oxygen in the discharge channels is low. However, there is an increased aluminium content in the inner areas of the coating. Therefore, the disadvantage of PEO coatings is a relatively large amount of electricity needed to form the coatings.

The purpose of this work is to analyse the process of synthesis of oxide ceramic coatings and to develop methods for their production, which would increase the rate of growth and, accordingly, reduce the energy consumption.

The formation of aluminium oxide in plasma discharges is described by the formulas:



Based on the law of the active masses it is possible to increase the yield of aluminium oxide by reactions (5-8) by increasing the concentrations of reagents, in particular O, O₂, OH, and OH⁻ [21].

It is important to investigate the effect of the addition of hydrogen peroxide on the phase composition, thickness, and porosity of the oxide ceramic coatings obtained on 2024 aluminium alloy by plasma electrolyte oxidation.

2. Experimental procedures

The oxide ceramic coatings were synthesized on 2024 aluminium alloy (94.7 wt.% Al, 3.8-4.9 wt.% Cu, 1.2-1.8% wt.% Mg, 0.3-0.9 wt.% Mn). The sample size was 20×15×3 mm. The samples were polished and washed in distilled water and ethyl alcohol before synthesis. The coatings were formed by the alternate application of anode and cathode pulses to the sample. Anode current density was $J_a = 10$ A/dm², and cathode current density was $J_c = 10$ A/dm². The electrolytes used in this work were aqueous solutions of KOH (3 g/l) and Na₂SiO₃ (2 g/l) without and with the addition of H₂O₂ (3 g/l), H₂O₂ (5 g/l), and H₂O₂ (7 g/l).

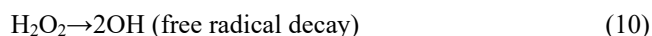
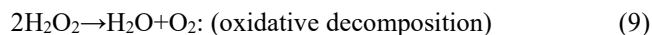
X-ray diffraction analysis of coatings was performed on a DRON-3.0 X-ray diffractometer using CuK_α radiation. The percentage of each phase was determined by the X-ray diffraction using the software package FullProf by Rietveld method.

The thickness of the coatings was determined using a CHY TG-05 thickness gauge (the measurement accuracy is $\pm 10 \mu\text{m} \pm 10\%$ for the range of 0-199 μm). The porosity of the coatings was investigated by analysing the micrographs of the PEO coatings obtained on a scanning electron microscope at $\times 500$ magnification using the technique [22]. In order to localize pores in the images we used a multiresolution relevance function [23]. The pore areas are selected using a local image function, which is calculated as difference between estimated intensities of background and object for the given scale. The next step is the analysis of the perimeter pixels for the region of interest. It allows to reject non compact objects that are not pores. The last step is local segmentation.

The number of pores, pores area, density of pores, ratio of pores area to the total area, average and maximum size of the pores were calculated after segmentation.

3. Results and discussion

The hydrogen peroxide molecule is capable of breaking down in two ways:



In the first case, the content of molecular oxygen will increase in the electrolyte, and in the second one, the OH radical will increase in the electrolyte. This will increase the yield of aluminium oxide by reactions (5-8).

Oxide ceramic coatings were synthesized for 1 h in the described above electrolytes. The optimal current densities were 20-30 A/dm². However, there is a problem of formation of coating on large areas (for this purpose, high current densities should be provided). Therefore, there is a problem of current parameters selection which will allow to form a coating at low power consumption (see Fig. 1).

It is known [19,24,25] that the maximum content of α -Al₂O₃ is formed in coatings after 2 h of synthesis. Oxide ceramic coatings synthesized in the electrolyte containing KOH (3 g/l) and Na₂SiO₃ (2 g/l) for 1 h and 2 h of synthesis were used to compare the results.

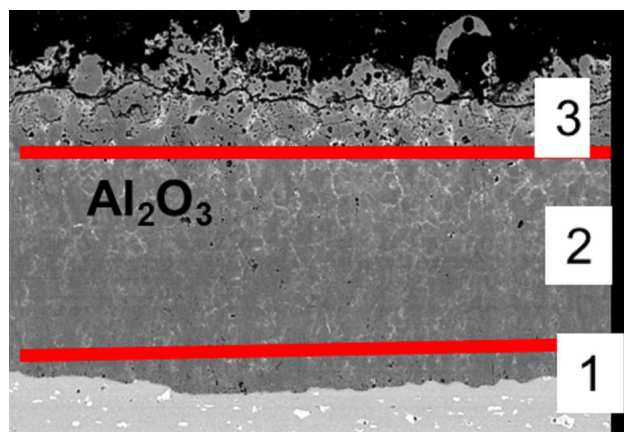


Fig. 1. Microstructure of an oxide ceramic coating after 2 h of synthesis in the electrolyte containing KOH (3 g/l) and Na₂SiO₃ (2 g/l): 1 – Al alloy substrate, 2 – working layer, 3 – technological layer

The phase compositions of the obtained coatings determined by the Rietveld multi-profile analysis using known structures of α -Al₂O₃ (R-3C) and γ -Al₂O₃ (Fd3m) [26,27] are presented in Figure 2.

The maximum content of α -Al₂O₃ (33.47%) in coatings is obtained within 2 h of synthesis in the original electrolyte (Fig. 2a, coating 2 in Tab. 1). Addition of 3 g/l H₂O₂ to this electrolyte makes it possible to obtain oxide ceramic coatings with a slightly smaller thickness and lower content of α -Al₂O₃ (29.34%) but within 1 h of synthesis (Fig. 2b, coating 3 in Tab. 1). A further increase in the concentration of hydrogen peroxide in the electrolyte (coating 4 in Tab. 1) allows to synthesize a coating that is almost as thick as coating 2 in Table 1, but such an increase in hydrogen peroxide leads to a decrease (up to 21.01%) in the amount of corundum (α -Al₂O₃). However, the advantage of this coating

in the amount of corundum remains as compared to the initial mode after synthesis for 1 h (coating 4 vs coating 1 in Tab. 1). At a concentration of 7 g/l H_2O_2 in the electrolyte, the amount of corundum continues to decrease (Fig. 2c, coating 5 in Tab. 1) and becomes commensurate with the amount of corundum in coating 1. However, the thickness of coating 5 is 1.5 times greater than coating 1 (Tab. 1).

Increasing the concentration of hydrogen peroxide leads to an increase in concentration of oxidizers and, accordingly, increases the thickness of the oxide ceramic coating. It was found that the optimal concentration of H_2O_2 in the electrolyte was 5 g/l. The coating synthesized in such electrolyte has a thickness of 109 μm , which is almost twice as much as in the coating formed in the original electrolyte for 1 h of synthesis. Hydrogen peroxide at a concentration of 3 g/l has almost no effect on the growth rate of the coating compared to coating 1. At a concentration of 7 g/l, the

growth rate of the coating is higher compared to coating 1, but lower compared to coating 4.

The porosity of the oxide ceramic coatings obtained in different electrolytes is slightly different and is 3.3-4.3%. With increasing the synthesis duration by two times the porosity decreases, while the maximum pore size increases slightly. Moreover, the maximum pore size is lower in the coatings obtained in the electrolyte containing KOH (3 g/l) and Na_2SiO_3 (2 g/l) within 1 h (see Fig. 3), than in the coatings obtained in the same electrolyte, but after 2 h of synthesis.

The reason for the increase of porosity is the increase of the power of plasma discharges, since over time their synthesis number of discharges decreases and the size increases.

It should be noted that the segmentation method (Fig. 3a) developed in [23] allows to detect pores clearly by analysing images (Fig. 3b) of surfaces.

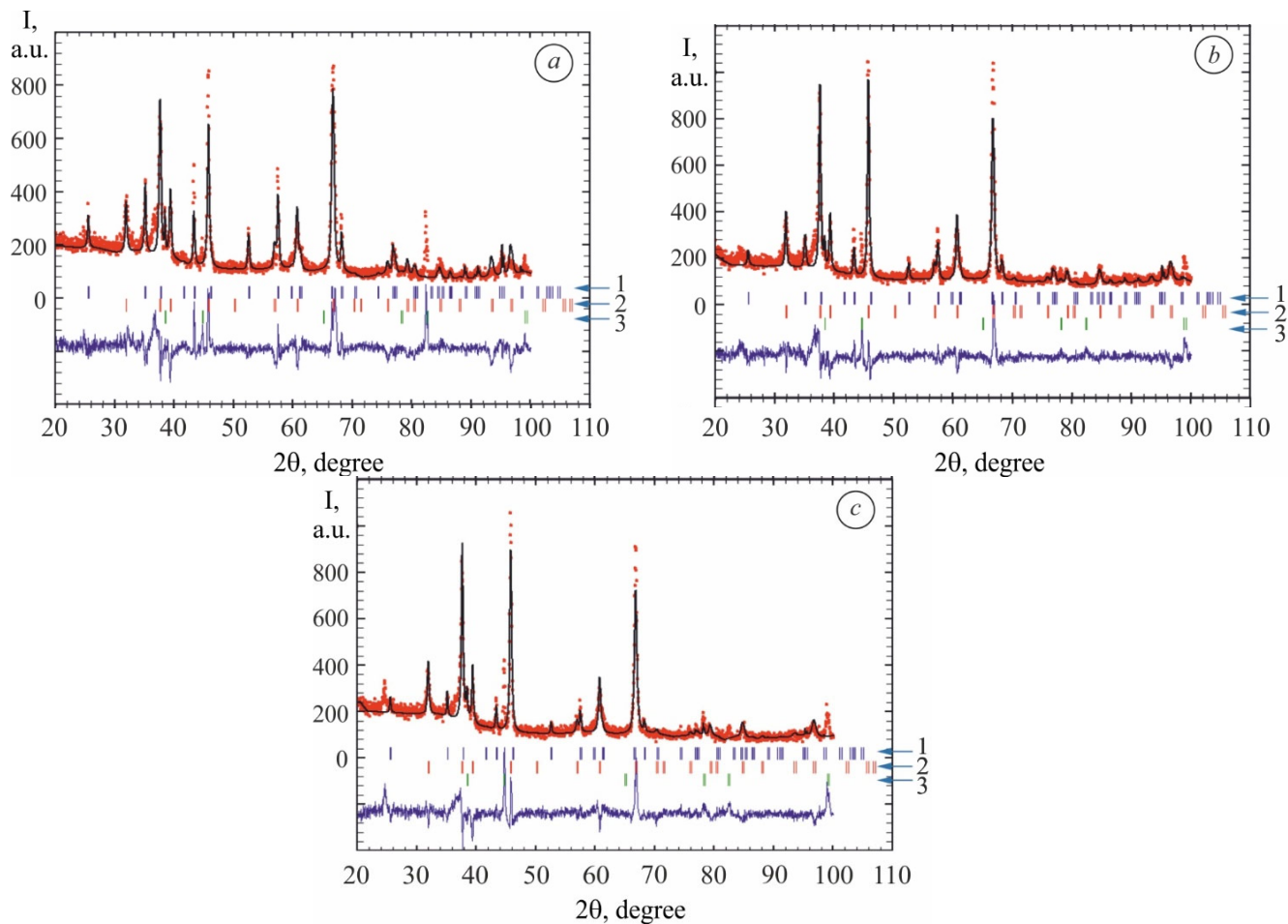


Fig. 2. X-ray diffraction patterns of oxide ceramic coating: $3KOH+2Na_2SiO_3$, $J_c/J_a = 10/10$ A/dm², $t=2$ h (a); $3KOH+2Na_2SiO_3+3H_2O_2$, $J_c/J_a=10/10$ A/dm², $t=1$ h (b), and $3KOH+2Na_2SiO_3+7H_2O_2$, $J_c/J_a = 10/10$ A/dm², $t=1$ h (c). Experimental (●), calculated (solid line), and the difference (bottom line) X-ray diffraction profiles. 1 – α - Al_2O_3 reflex, 2 – γ - Al_2O_3 reflex, 3 – Al reflex

Table 1. Phase composition, thickness, and modes of synthesis of the obtained coatings

Coating	Phase, %			Oxidizer	Synthesis time, h	J_c/J_a , A/dm ²	Thickness, μm	Porosity, %	Max. pore size, μm^2
	$\alpha\text{-Al}_2\text{O}_3$	$\gamma\text{-Al}_2\text{O}_3$	Al						
1	16.15	71.74	12.11	3KOH+2Na ₂ SiO ₃	1	10/10	63	4.32	1.434·10 ²
2	33.47	64.46	2.07	3KOH+2Na ₂ SiO ₃	2	10/10	115	3.95	1.494·10 ²
3	29.34	62.71	7.95	3KOH+2Na ₂ SiO ₃ +3H ₂ O ₂	1	10/10	74	3.55	0.996·10 ²
4	21.01	76.53	2.46	3KOH+2Na ₂ SiO ₃ +5H ₂ O ₂	1	10/10	109	3.53	0.594·10 ²
5	15.54	81.20	3.26	3KOH+2Na ₂ SiO ₃ +7H ₂ O ₂	1	10/10	91	3.37	0.448·10 ²

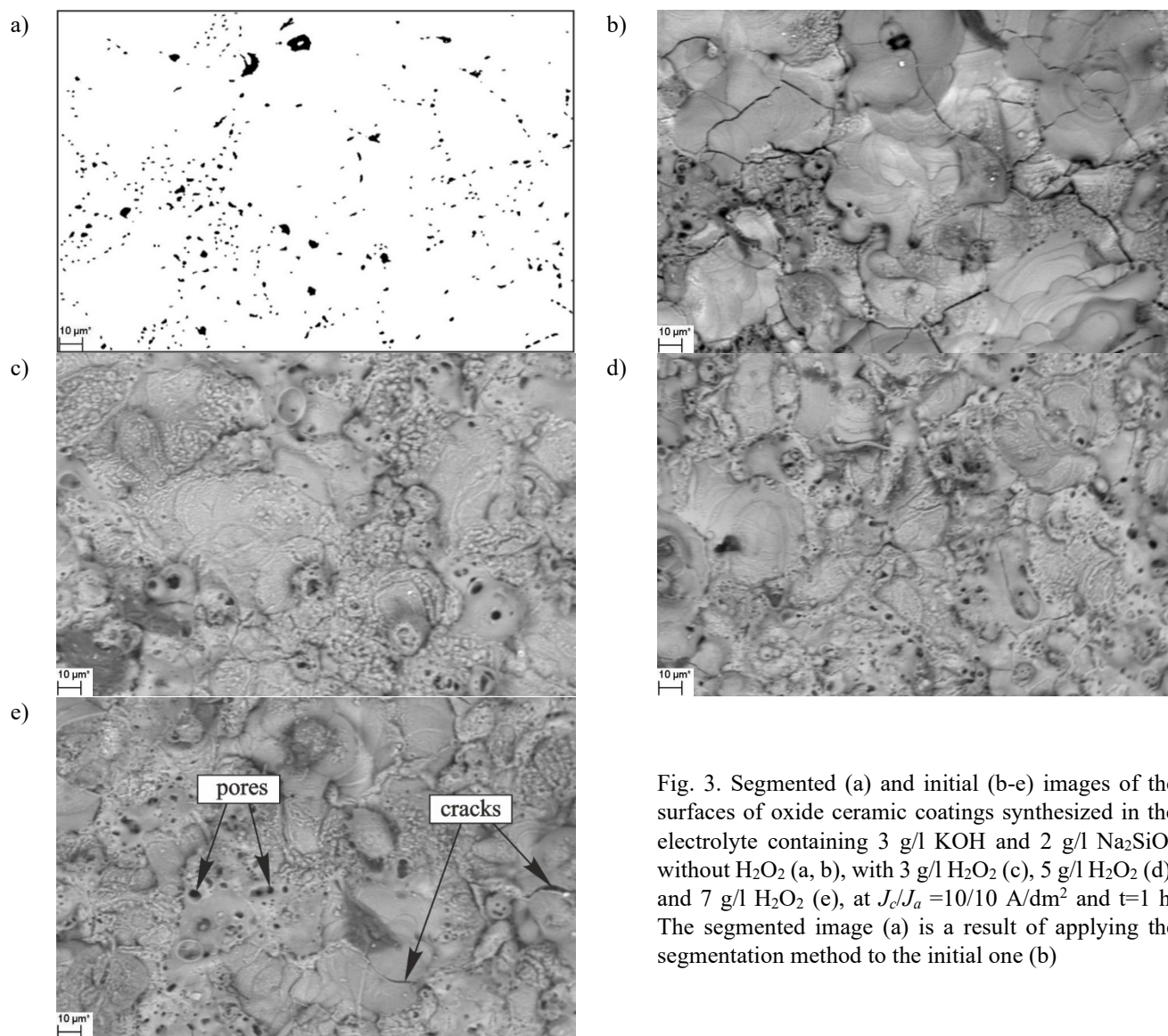


Fig. 3. Segmented (a) and initial (b-e) images of the surfaces of oxide ceramic coatings synthesized in the electrolyte containing 3 g/l KOH and 2 g/l Na₂SiO₃ without H₂O₂ (a, b), with 3 g/l H₂O₂ (c), 5 g/l H₂O₂ (d), and 7 g/l H₂O₂ (e), at $J_c/J_a=10/10$ A/dm² and $t=1$ h. The segmented image (a) is a result of applying the segmentation method to the initial one (b)

It is seen from Fig. 3 and the porosity data presented in Table 1 that on the surface of the oxide ceramic coatings synthesized in the 3KOH+2Na₂SiO₃ electrolyte, there are

pores and a large number of cracks. The addition of 3 and 5 g/l of hydrogen peroxide to the electrolyte leads to the formation of a continuous coating without cracks and a

decrease in porosity from 4.32% (Fig. 3b, coating 1 in Table 1) to 3.55% (Fig. 3c, coating 3) and 3.53% (Fig. 3d, coating 4), respectively. Besides, the maximum pore size is reduced by 1.4 and 2.4 times after the addition of 3 and 5 g/l of hydrogen peroxide, respectively.

With a further increase in the concentration of hydrogen peroxide to 7 g/l, the porosity and maximum pore size are slightly reduced, but the thickness of the synthesized coating decreases more significantly as compared to coating 4. Besides, application of this mode of synthesis (coating 5 in Table 1) leads to microcracking the synthesized coating (Fig. 3e, coating 5).

Although the number of pores in the obtained coatings is large, not all of them are through and reach the base metal and, accordingly, do not take part in the corrosion processes.

In order to continue optimizing the synthesis of oxide ceramic coatings, it is necessary to investigate the relationship between phase composition and porosity or through-porosity of coatings with the physical and mechanical properties and corrosion resistance. Since these coatings have found their application in parts that work in abrasive wear condition, it is need to conduct the micro-hardness, microplasticity, and wear resistance studies and reveal the relationship between corresponding parameters. Besides, to expand the range of application of the obtained coatings, it is necessary to investigate their corrosion resistance in different environments, through porosity, and choose the methods of increasing their corrosion resistance.

4. Conclusions

- The analysis of the process of plasma electrolyte synthesis of oxide ceramic coatings on 2024 aluminium alloy (94.7 wt.% Al, 3.8-4.9 wt.% Cu, 1.2-1.8% wt.% Mg, 0.3-0.9 wt.% Mn) in the electrolyte containing KOH (3 g/l) and Na₂SiO₃ (2 g/l) has been performed. Methods for accelerating the coating formation have been proposed and tested, in particular, by adding various concentrations of H₂O₂ to the electrolyte. The content of α-Al₂O₃ and γ-Al₂O₃ oxides in the obtained coatings was determined by X-ray phase analysis, in particular, their ratios at various concentrations of H₂O₂ in the electrolyte.
- The addition of 3–5 g/l of hydrogen peroxide to the 3KOH+2Na₂SiO₃ electrolyte leads to the formation of a continuous coating without cracks and a decrease in porosity from 4.32% to 3.55–3.53%. The maximum pore size is reduced by 1.4 and 2.4 times after the addition of 3 and 5 g/l of hydrogen peroxide, respectively.
- The oxide ceramic coating synthesized in the 3KOH+2Na₂SiO₃ electrolyte with 7 g/l H₂O₂ additive contains microcracks. The thickness of the synthesized coating is reduced as compared to a coating synthesized in the 3KOH+2Na₂SiO₃ electrolyte with 5 g/l H₂O₂.
- We have selected the electrolyte with 5 g/l H₂O₂ additive as an optimal composition for synthesis of a coating with an increased content of corundum (α-Al₂O₃) as compared to a coating synthesized in the same mode in the 3KOH+2Na₂SiO₃ electrolyte without H₂O₂.

References

- L.A. Dobrzański, L.B. Dobrzański, A.D. Dobrzańska-Danikiewicz, Manufacturing technologies thick-layer coatings on various substrates and manufacturing gradient materials using powders of metals, their alloys and ceramics, *Journal of Achievements in Materials and Manufacturing Engineering* 99/1 (2020) 14-41. DOI: <https://doi.org/10.5604/01.3001.0014.1598>
- G.W. Critchlow, K.A. Yendall, D. Bahrani, A. Quinn, F. Andrews, Strategies for the replacement of chromic acid anodizing for the structural bonding of aluminium alloys, *International Journal of Adhesion and Adhesives* 26/6 (2006) 419-453. DOI: <https://doi.org/10.1016/j.ijadhadh.2005.07.001>
- K. Szymkiewicz, J. Morgiel, L. Maj, M. Pomorska, M. Tarnowski, O. Tkachuk, I. Pohrelyuk, T. Wierzchoń, Effect of nitriding conditions of Ti₆Al₇Nb on microstructure of TiN surface layer, *Journal of Alloys and Compounds* 845 (2020) 156320. DOI: <https://doi.org/10.1016/j.jallcom.2020.156320>
- S.A. Abdel-Gawad, W. Osman, A. Fekry, Characterization and corrosion behavior of anodized Aluminum alloys for military industries applications in artificial seawater, *Surfaces and Interfaces* 14 (2019) 314-323. DOI: <https://doi.org/10.1016/j.surfin.2018.08.001>
- Z.A. Duriagina, T.M. Kovbasyuk, S.A. Bespalov, The analysis of competitive methods of improvement of operational properties of functional layers of flat heating elements, *Uspehi Fiziki Metallov* 17 (2016) 29-51. DOI: <https://doi.org/10.15407/ufm.17.01.029>
- V.G. Efremenko, K. Shimizu, T.V. Pastukhova, Y.G. Chabak, K. Kusumoto, A.V. Efremenko, Effect of bulk heat treatment and plasma surface hardening on the microstructure and erosion wear resistance of complex-alloyed cast irons with spheroidal vanadium carbides, *Journal of Friction and Wear* 38/1 (2017) 58-64. DOI: <https://doi.org/10.3103/S1068366617010056>
- L. Ropyak, V. Ostapovych, Optimization of process parameters of chrome plating for providing quality indicators of reciprocating pumps parts, *Eastern-European Journal of Enterprise Technologies* 2 (2016) 50-62. DOI: <https://doi.org/10.15587/1729-4061.2016.65719>
- M.M. Student, V.V. Shmyrko, M.D. Klapkiv, I.M. Lyasota, L.N. Dobrovolska, Evaluation of the mechanical properties of combined metal-oxide-ceramic layers on aluminum alloys, *Materials Science* 50 (2014) 290-295. DOI: <https://doi.org/10.1007/s11003-014-9720-9>

- [9] A.L. Yerokhin, X. Nie, A. Leyland, A. Matthews, S.J. Dowey, Plasma electrolysis for surface engineering, *Surface and Coatings Technology* 122 (1999) 73-93. DOI: [https://doi.org/10.1016/S0257-8972\(99\)00441-7](https://doi.org/10.1016/S0257-8972(99)00441-7)
- [10] X. Nie, E.I. Meletis, J.C. Jiang, A. Leyland, A.L. Yerokhin, A. Matthews, Abrasive wear/corrosion properties and TEM analysis of Al₂O₃ coatings fabricated using plasma electrolysis, *Surface and Coatings Technology* 149 (2002) 245-251. DOI: [https://doi.org/10.1016/S0257-8972\(01\)01453-0](https://doi.org/10.1016/S0257-8972(01)01453-0)
- [11] M.M. Student, V.M. Dovhnyk, M.D. Klapkiv, V.M. Posuvailo, V.V. Shmyrko, A.P. Kytsya, Tribological properties of combined metal-oxide-ceramic layers on light alloys, *Materials Science* 48 (2012) 180-190 DOI: <https://doi.org/10.1007/s11003-012-9489-7>
- [12] M.-G. Park, H.-C. Choe, Functional elements coatings on Ti-6Al-4V alloy by plasma electrolytic oxidation for biomaterials, *Journal of Nanoscience and Nanotechnology* 19/2 (2019) 1114-1117. DOI: <https://doi.org/10.1166/jnn.2019.15903>
- [13] S.-Y. Park, H.-C. Choe, Functional element coatings on Ti-alloys for biomaterials by plasma electrolytic oxidation, *Thin Solid Films* 699 (2020) 137896. DOI: <https://doi.org/10.1016/j.tsf.2020.137896>
- [14] Y. Cheng, Q. Zhang, Z. Zhu, W. Tu, Y. Cheng, P. Skeldon, Potential and morphological transitions during bipolar plasma electrolytic oxidation of tantalum in silicate electrolyte, *Ceramics International* 46/9 (2020) 13385-13396. DOI: <https://doi.org/10.1016/j.ceramint.2020.02.120>
- [15] R. Chaharmahali, A. Fattah-alhosseini, K. Babaei, Surface characterization and corrosion behavior of calcium phosphate (Ca-P) base composite layer on Mg and its alloys using plasma electrolytic oxidation (PEO): A review, *Journal of Magnesium and Alloys* (2020) (in press). DOI: <https://doi.org/10.1016/j.jma.2020.07.004>
- [16] M.D. Klapkiv, Simulation of synthesis of oxide-ceramic coatings in discharge channels of a metal-electrolyte system, *Materials Science* 35 (1999) 279-283. DOI: <https://doi.org/10.1007/BF02359992>
- [17] B. Kasalica, M. Petković-Benazzouz, M. Sarvan, I. Belča, B. Maksimović, B. Misailović, Z. Popović, Mechanisms of plasma electrolytic oxidation of aluminum at the multi-hour timescales, *Surface and Coatings Technology* 390 (2020) 125681. DOI: <https://doi.org/10.1016/j.surfcoat.2020.125681>
- [18] M.D. Klapkiv, N.Yu. Povstyana, H.M. Nykyforchyn, Production of conversion oxide-ceramic coatings on zirconium and titanium alloys, *Materials Science* 42 (2006) 277-286 DOI: <https://doi.org/10.1007/s11003-006-0081-x>
- [19] V. Dehnavi, X.Y. Liu, B.L. Luan, D.W. Shoesmith, S. Rohani, Phase transformation in plasma electrolytic oxidation coatings on 6061 aluminum alloy, *Surface and Coatings Technology* 251 (2014) 106-114. DOI: <https://doi.org/10.1016/j.surfcoat.2014.04.010>
- [20] L.A. Snezhko, A.L. Erokhin, O.A. Kalinichenko, D.A. Misnyankin, Hydrogen release on the anode in the course of plasma electrolytic oxidation of aluminum, *Materials Science* 52 (2016) 421-430. DOI: <https://doi.org/10.1007/s11003-016-9974-5>
- [21] M.D. Klapkiv, O.S. Chuchmarev, P.Ya. Sydor, V.M. Posuvailo, Thermodynamics of the interaction of aluminum, magnesium, and zirconium with components of an electrolytic plasma, *Materials Science* 36 (2000) 66-79. DOI: <https://doi.org/10.1007/BF02805119>
- [22] M.M. Student, I.B. Ivasenko, V.M. Posuvailo, H.H. Veselivs'ka, A.Y. Pokhmurs'kyi, Y.Y. Sirak, V.M. Yus'kiv, Influence of the porosity of a plasma-electrolytic coating on the corrosion resistance of D16 alloy, *Materials Science* 54 (2019) 899-906. DOI: <https://doi.org/10.1007/s11003-019-00278-z>
- [23] I.B. Ivasenko, V.M. Posuvailo, M.D. Klapkiv, V.A. Vynar, S.I. Ostap'yuk, Express method for determining the presence of defects of the surface of oxide-ceramic coatings, *Materials Science* 45 (2009) 460-464. DOI: <https://doi.org/10.1007/s11003-009-9191-6>
- [24] X. Shi-Gang, S. Li-Xin, Z. Rong-Gen, H. Xing-Fang, Properties of aluminium oxide coating on aluminium alloy produced by micro-arc oxidation, *Surface and Coatings Technology* 199 (2005) 184-188. DOI: <https://doi.org/10.1016/j.surfcoat.2004.11.044>
- [25] J. Martin, P. Leone, A. Nominé, D. Veys-Renaux, G. Henrion, T. Belmonte. Influence of electrolyte ageing on the plasma electrolytic oxidation of aluminium, *Surface and Coatings Technology* 269 (2015) 36-46. DOI: <https://doi.org/10.1016/j.surfcoat.2014.11.001>
- [26] L.W. Finger, R.M. Hazen, Crystal structure and compression of ruby to 46 kbar, *Journal of Applied Physics* 49 (1978) 5823-5826. DOI: <https://doi.org/10.1063/1.324598>
- [27] K. Liddell, Univ. of Newcastle, Dept. of Mechanical, Materials and Manufacturing Engineering, England, UK, Private Communication, 1996.



© 2020 by the authors. Licensee International OCSCO World Press, Gliwice, Poland. This paper is an open access paper distributed under the terms and conditions of the Creative Commons Attribution-NonCommercial-NoDerivatives 4.0 International (CC BY-NC-ND 4.0) license (<https://creativecommons.org/licenses/by-nc-nd/4.0/deed.en>).